atmosphere

MDPI

Article

Spatio-Temporal Variation and Influencing Factors of Ozone Pollution in Beijing

Bo Chen [1,*], Xinbing Yang [2] and Jingjing Xu [2,*]

[1] Institute of Forestry and Pomology, Beijing Academy of Agriculture and Forestry Sciences, Beijing 100093, China
[2] College of Forestry, Hebei Agriculture University, Baoding 071001, China; hbyxb2008@126.com
* Correspondence: zhyechb2010@163.com (B.C.); x16603297326@163.com (J.X.)

Abstract: The temporal and spatial distribution and variation characteristics of ozone (O_3) in Beijing, China, are investigated using hourly monitoring data from 2020. Kriging interpolation analysis and correlation analysis are applied to describe the spatial-temporal distribution and to identify associated influencing factors. The average concentration of O_3 was found to be 59.58 $\mu g \cdot m^{-3}$. The daily maximum sliding 8 h average ozone concentration values exceeded the primary standard (100 $\mu g \cdot m^{-3}$) for 129 days and exceeded the secondary standard (160 $\mu g \cdot m^{-3}$) for 48 days. Temporally, the general pattern of daily maximum 8 h average O_3 concentration was high in spring and summer and low in autumn and winter. Monthly average values showed a maximum in June. The highest daily concentrations appeared between 13:00 and 18:00 local time, and O_3 concentrations had a distinct weekly pattern of variability with daily average concentrations at weekends higher than those during working days. Spatially, annual average O_3 concentrations were highest in the northeast and lowest in the southeast of the city, and the seasonal variation of O_3 was most significant in the southwest of the city. In relation to city districts and counties, the annual average O_3 concentrations in the Miyun District were the highest, while those in the Haidian District were the lowest. On the whole, annual average O_3 concentrations in Beijing were higher in the suburbs than in central areas. Based on daily average values, there was no significant correlation between O_3 concentrations and rainfall ($p > 0.05$), but there were significant correlations between O_3 concentration and sunshine hours, wind speed, maximum temperature and minimum temperature ($p < 0.05$), with correlation coefficients of 0.158, 0.267, 0.724 and 0.703, respectively. O_3 concentrations increased with an increasing number of sunshine hours, first increased and then decreased with increasing wind speed and increased with increasing temperature. O_3 concentrations were correlated with SO_2 concentrations ($0.05 < p > 0.001$), CO concentrations ($p < 0.001$) and NO_2 concentrations ($p < 0.001$), the latter having the highest correlation coefficient of -0.553 and exhibiting opposite trends in daily and monthly variations to O_3 variations. Analysis of ozone pollution sources showed that automobile exhaust, coal and oil combustion and volatile organic compounds released by industrial plants were the main sources. Terrain affected the distribution of ozone, as well as human activities and industry.

Keywords: ozone pollution; spatio-temporal variation; urban areas; causative factors

Citation: Chen, B.; Yang, X.; Xu, J. Spatio-Temporal Variation and Influencing Factors of Ozone Pollution in Beijing. *Atmosphere* **2022**, *13*, 359. https://doi.org/10.3390/atmos13020359

Academic Editors: Yiming Liu, Oleg Romanovskii and Hyung-Min Lee

Received: 31 December 2021
Accepted: 17 February 2022
Published: 21 February 2022

1. Introduction

Ozone (O_3) is an important component of the atmosphere, most of which lies in the stratosphere, and a small part exists in the troposphere. Stratospheric O_3 can protect terrestrial organisms from radiation hazards by absorbing external ultraviolet radiation. As a greenhouse gas, O_3 can absorb solar radiation reflected from the ground and re-emit the radiation, hence contributing to global warming and climatic change [1]. The precursors

of tropospheric O_3 are generally nitrogen oxides (NO_x) and volatile organic compounds (VOC_s) [2]. The reaction process is as follows:

$$\left.\begin{matrix} CO \\ VOC_s \end{matrix}\right\} + NO_x \xrightarrow{\text{Solar radiation}} O_3 \quad (1)$$

The formation process of O_3 is extremely nonlinear [3]. The increase of O_3 concentrations in the troposphere can potentially affect the health of human beings, animals and plants. In a high-concentration O_3 environment, human beings are prone to respiratory diseases and the growth and output of crops are inhibited [4]. In Beijing, China, control experiments in an open-top chamber (OTC) with different O_3 concentrations showed that with increasing O_3 concentrations, the biomass of trees decreased significantly, the net photosynthetic rate and transpiration rate decreased, the intercellular carbon dioxide concentration increased and the chlorophyll content, stomatal area and stomatal opening were also affected [5]. Leaves became sapless, yellow, even died. In addition, the root biomass, fine root yield, turnover and underground carbon availability of trees decreased [6]. Hence high O_3 concentrations can cause agricultural and forestry industries to reduce their production and reduce their economic outputs.

Monitoring O_3 concentration is an important task for controlling air pollution [7]. The composition of the atmosphere is influenced by the development of industrialization and urbanization and the enhancement of human activities. The atmospheric content of sulfur dioxide (SO_2), nitrogen oxides (NO_x), ozone (O_3), respirable particulate matter (PM_{10}) and respirable particulate matter ($PM_{2.5}$) are constantly increasing. Air pollution has become a serious problem endangering human health and the survival of animals and plants.

In recent years, human activities have greatly increased the O_3 precursors discharged into the atmosphere, creating conditions for increasing O_3 concentrations. Pollution caused by O_3 is serious in urban areas, especially in the Beijing-Tianjin-Hebei, Yangtze River Delta and Pearl River Delta urban agglomerations in China [8–10]. In 2019, $PM_{2.5}$, PM_{10}, SO_2, NO_2 and CO in 338 prefecture-level cities all declined in part, while only O_3 concentration increased by 6.5% year-on-year [11]. Restrictions on nitrogen oxides emissions have achieved remarkable results, but VOCs have been increasing. Many countries in the world actively respond to O_3 pollution. They have shown that single control of volatile organic compounds (VOCs), coordinated control of VOCs and NOx, local controls and regional coordinated prevention initiatives can all achieve remarkable results [12]. However, at present, China mainly adopts comprehensive control measures, such as monitoring, early warning and limiting the discharge of precursors [13].

Previous studies have shown that there are daily and weekly cycles of ozone and local ozone concentrations can be influenced by upwind transport [14], weekly cycles of VOCs/NOx and aerosol concentrations [15], as well as the surrounding environment [16,17]. Furthermore, the seasonal cycle of O_3 is significant [18,19]. Changes in ozone precursor emissions [20], synoptic weather [21], summer monsoon and farmland biomass burning [22] have all been shown to influence the seasonal cycle of ozone. Research conducted in southern California [23], Los Angeles [24], New York [25] and their surrounding areas [26] have demonstrated the weekly cycle of urban O_3. On a daily timescale, O_3 usually presents a unimodal characteristic [27], and some studies have used the daily cycle as the standard against which to test the simulation effect of O_3 models.

The main factors affecting the spatial distribution characteristics of O_3 include the presence of precursors in different regions, differences in photochemical reaction conditions and transport from adjacent sources. For example, Haiying found that there are two O_3 pollution zones in Beijing, one mainly concentrated in Beijing-Baoding-northwestern Shanxi, and the other in Beijing-Tianjin-Bohai [28]. In recent years, research has focused on the distribution of $PM_{2.5}$, PM_{10} and NO_2, although the natural and anthropogenic environmental conditions within cities will also determine the spatial characteristics of air pollution [29].

The variation in O_3 concentrations and distribution is of great significance to urban ecological planning and environmental governance. In 2020, the concentration of ozone in Beijing exceeded the national secondary standard by 9.0%, while other pollutants (SO_2, NO_2, PM_{10} and $PM_{2.5}$) were all found to be decreasing. Beijing, as the capital of China, is the pioneer area demonstrating ecological urban planning and governance. Hence, it is urgent to control air pollution in the city and improve the quality of the environment. In order to achieve this, a systematic study of the temporal variation and spatial distribution of ozone pollution in Beijing is needed, as well as an investigation of the relationship between O_3 spatial-temporal patterns, climatic conditions and other pollutants in Beijing.

This study uses hourly O_3 concentration data from 35 atmospheric monitoring stations within Beijing in 2020 to investigate the temporal and spatial distribution of O_3. Meteorological data is used to explore the relationship between ozone concentrations and meteorological conditions and to investigate the critical factors that affect local air quality. The purpose is to better understand the factors influencing O_3 pollution in Beijing in order to provide evidence for the formulation of improved pollution-control policies.

2. Materials and Methods

2.1. The Research Area

Beijing (115.7–117.4° E, 39.4–41.6° N) is located in the northwest of the North China Plain and is surrounded by mountains on three sides, making it difficult for polluted gases to naturally diffuse. The altitude of the Beijing Plain is 20–60 m, and the altitude of the surrounding mountainous areas is generally 1000–1500 m. The regional climate belongs to the warm temperate zone, with four distinct seasons: long winters and summers, short springs and autumns. There is moderate precipitation, long frost-free periods and the annual average temperature is 8–12 °C. The annual average precipitation is about 600 mm, and the seasonal distribution of precipitation is very uneven. A total of 70% of the annual rainfall is concentrated in July, August and September. Forest coverage is about 43.5% in Beijing by area and about 28.5% on the North China Plain. The urban greening areal coverage is about 48.4%.

2.2. Data Sources and Analysis

Ozone monitoring data came from 35 monitoring points operated by the Beijing Environmental Protection Monitoring Center (Figure 1). The sites were categorized as follows: 23 urban environmental assessment sites; 6 regional transmission sites; 5 traffic pollution monitoring sites; and 1 urban clean control site. By geographical location, they were divided between six central districts (17 sites), the northwest of the city center (4 sites), the southwest (3 sites), the northeast (6 sites) and the southeast (5 sites). The data collection period was from January to December 2020.

O_3 was monitored using 49C ultraviolet O_3 analyzers produced by Thermo Fisher (an American thermoelectric environmental instrument company). The lowest detection limit of the O_3 analyzer was 1 ppb, the accuracy was ±1 ppb, the zero drift was 0.4%/24 h and the span drift was 1%/24 h and 2%/7 d.

NO_2 concentration was monitored using Thermo Fisher 42C chemiluminescence NO-NO_2-NO_x analyzers. The lowest detection limit of this analyzer was 0.05 ppb, the zero drift was less than 0.025×10^{-9}/24 h and the span drift was 1%/24 h.

CO concentration was measured using Thermo Fisher 48C analyzers based on the gas filtering infrared absorption method. SO_2 was monitored using T E-43C analyzers, employing the ultraviolet fluorescence method.

Meteorological data came from the Beijing meteorological station (No. 54511) and included precipitation, sunshine hours, wind speed, wind direction and maximum/minimum temperature data.

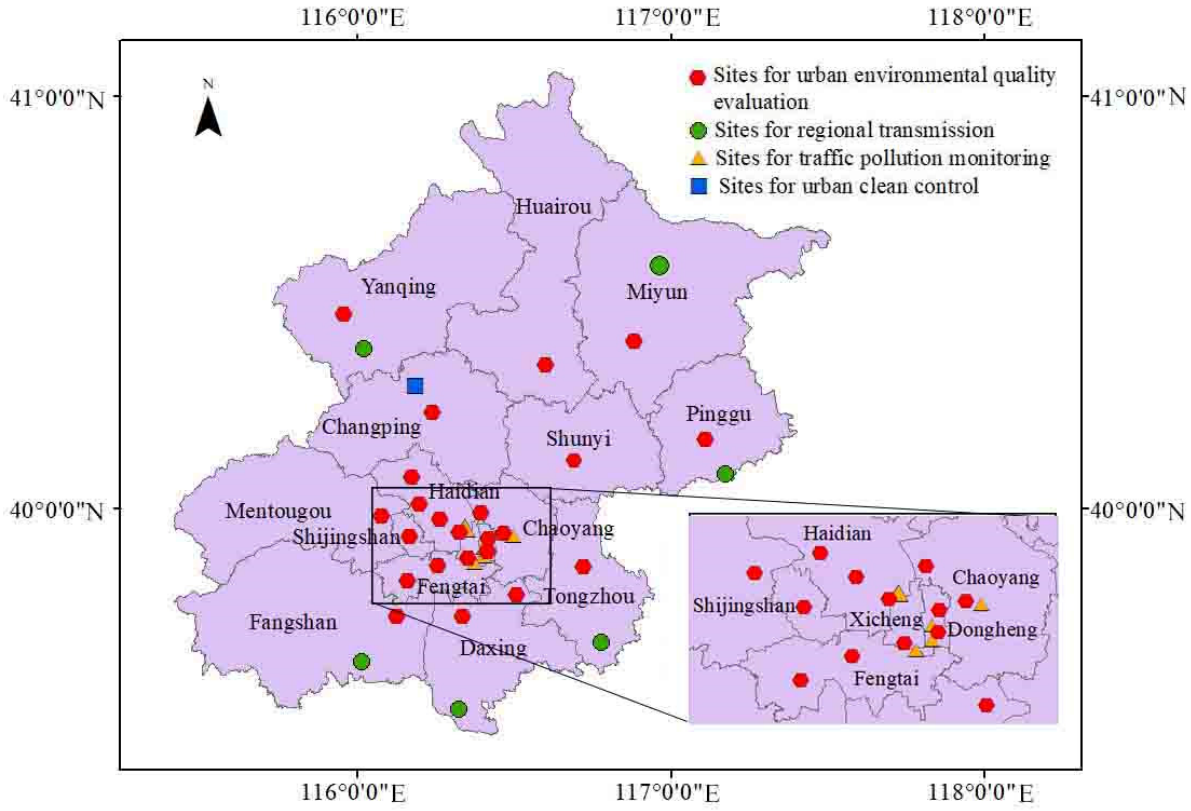

Figure 1. Map of the study area showing the location of the O_3 monitoring stations.

In this study, hourly data of O_3 concentration were selected for analysis, and classified on seasonal (monthly), daily and weekly time scales. Spatial analysis was carried out using the geographical categories of urban areas, northeast, northwest, southeast and southwest areas and 16 administrative central areas.

Kriging is an advanced geostatistical procedure that generates an estimated surface from a scattered set of points with values. Kriging methods were used to generate O_3 distribution maps based on the monitoring data. Data processing, Kriging interpolation analysis of O_3 concentrations and Pearson correlation analysis were carried out using Excel 2010, Arc GIS and SPSS software, respectively.

3. Results

3.1. Temporal Variation

The annual average value of O_3 concentration in Beijing was 59.58 $\mu g \cdot m^{-3}$, and the annual average daily maximum 8 h average concentration was 93.59 $\mu g \cdot m^{-3}$ although this demonstrated significant seasonal variation. With reference to the China Ambient Air Quality Standard (GB 3095—2012) [30], in 2020, the daily maximum 8 h average O_3 concentration exceeded the primary standard (100 $\mu g \cdot m^{-3}$) for 129 days and the secondary standard (160 $\mu g \cdot m^{-3}$) for 48 days. The highest daily maximum 8 h average in 2020 was 271.91 $\mu g \cdot m^{-3}$. The hourly average O_3 concentration exceeded the primary standard (160 $\mu g \cdot m^{-3}$) for 408 h and the secondary standard (200 $\mu g \cdot m^{-3}$) for 103 h. The highest 2020 value of the hourly average O_3 concentration was 297.03 $\mu g \cdot m^{-3}$.

The monthly average O_3 concentration (Figure 2) increased from January to June (cumulative increase of 238.6%), reached a peak value in June (111.73 $\mu g \cdot m^{-3}$) and then declined to the end of the year. The rate of increase from March to April (+43.2%) was larger than the rate of increase from May to June (+38.7%). The lowest concentrations in January and December were 23.45 and 25.79 $\mu g \cdot m^{-3}$, respectively.

In terms of the daily maximum 8 h average O_3 concentration, the highest values occurred in May to October (Figure 3). The seasonal order of the average O_3 concentration

in Beijing in 2020 was as follows: summer (95.04 μg·m^{-3}) > spring (72.99 μg·m^{-3}) > autumn (36.94 μg·m^{-3}) > winter (35.10 μg·m^{-3}). Hence the general pattern of daily maximum 8 h average O_3 concentration was high in spring and summer and low in autumn and winter.

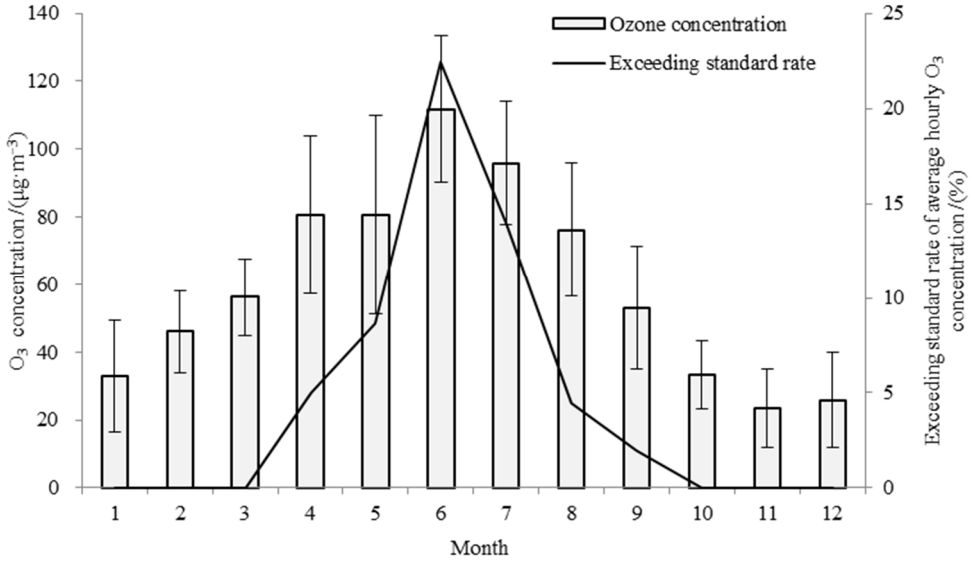

Figure 2. Annual variation of monthly average O_3 concentration.

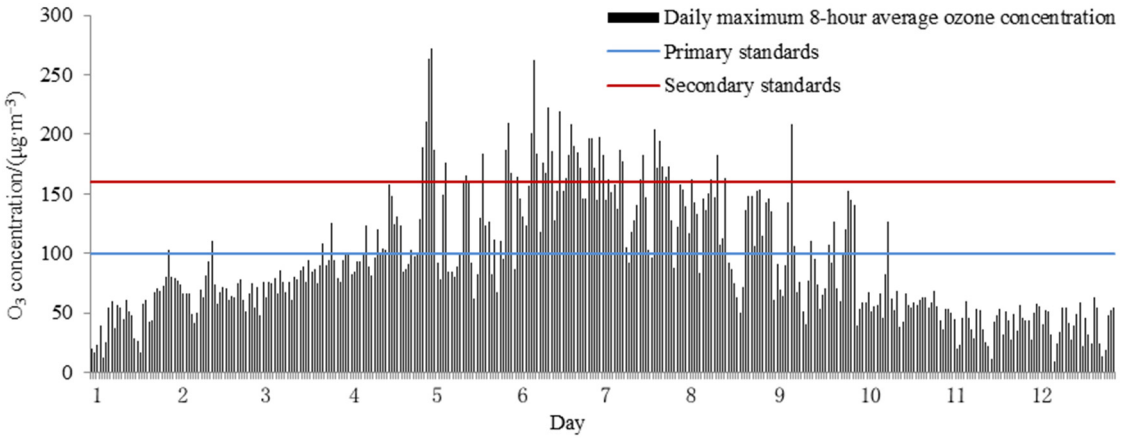

Figure 3. Annual variation of the daily maximum 8 h average ozone concentration. (Note: month value is plotted at the start of each month).

There was a significant diurnal variation of O_3 concentration (Figure 4), with a similar diurnal pattern of O_3 concentration in all four seasons, i.e., low in the early morning, high in the afternoon. The average across all monitoring stations in the city exhibited a peak value of O_3 concentration between 13:00 and 18:00, and minimum values between 01:00 and 08:00 and 19:00 and 24:00.

The diurnal variation in each of the four annual seasons was slightly different. Compared with autumn and winter, the daily peaks in spring and summer were later in the day, i.e., 15:00 in autumn and winter and 17:00 in spring and summer. In addition, the fluctuation of O_3 concentration was more significant in spring and summer and less in autumn and winter, especially at night. Hourly average O_3 concentrations in summer were higher than those in other seasons, followed by those in spring. Average O_3 concentrations in autumn were slightly lower than those in winter between 00:00 and 08:00, but higher in other time periods.

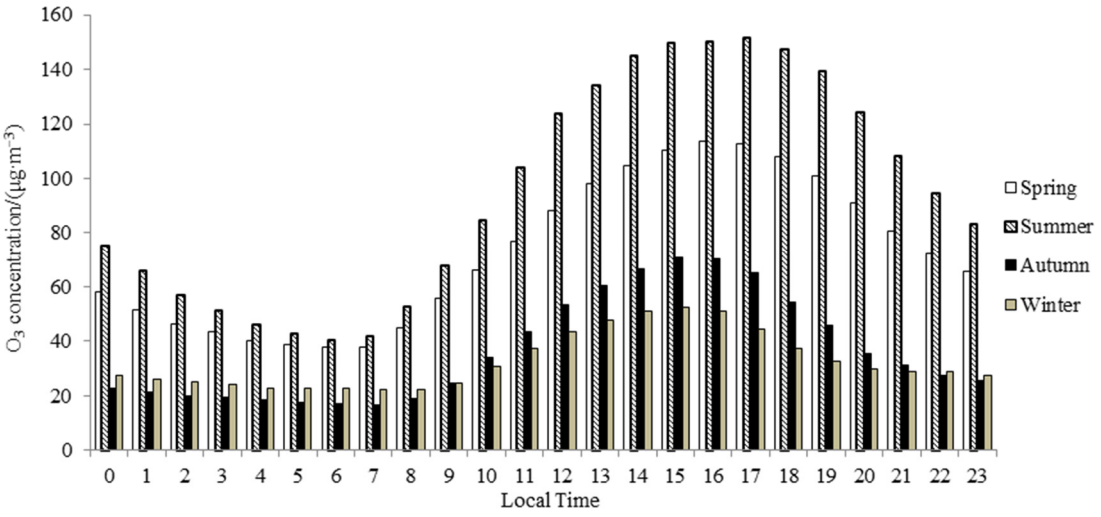

Figure 4. Diurnal variation of hourly O_3 concentration in the four annual seasons.

There was a clear weekly trend of daily mean O_3 concentrations (Table 1). Daily average O_3 concentrations in Beijing were at high levels on Fridays (61.37 ± 26.89 μg·m^{-3}), Saturdays (61.46 ± 27.18 μg·m^{-3}) and Sundays (61.05 ± 23.83 μg·m^{-3}). In the spring, the concentrations of O_3 were highest on Thursdays and Fridays, and the lowest on Mondays, with the highest difference being 93.52%. The highest average values of daily mean O_3 concentration in summer appeared on weekends, although the higher values in autumn and winter appeared on Sundays and Mondays.

On the whole, average daily mean values on weekends were generally higher than those from working days. By selecting consecutive days (non-holidays) with similar weather conditions in representative months for analysis, it was found that the daily mean O_3 concentration of weekends in Beijing was generally higher than those of working days, with the lowest daily average O_3 concentrations on Wednesdays and Thursdays and highest on Saturdays and Sundays. Weekend restrictions in Beijing have led to the greater use of motor vehicles than during working days. This may increase the emission of O_3 precursors and may also closely result in changes to the surrounding climate and environment. Within Beijing's 5th Ring Road, motor vehicles are restricted according to the last number of their license plate. For example, vehicles with tail numbers 1 and 6, 2 and 7, 3 and 8, 4 and 9, 5 and 0 are banned on Monday, Tuesday, Wednesday, Thursday and Friday, respectively. However, there are no restrictions at weekends. Therefore, on working days, public transport is more heavily used than at weekends. This most likely reduces the emission of ozone precursors during the week to some extent.

Table 1. Weekly variation of daily mean O_3 concentration (μg·m^{-3}).

Time	Spring	Summer	Autumn	Winter	Average
Monday	59.07 ± 9.36	89.46 ± 13.92	42.33 ± 19.36	39.28 ± 8.32	57.54 ± 19.91
Tuesday	70.58 ± 8.63	91.84 ± 11.46	30.83 ± 11.78	37.30 ± 10.81	57.64 ± 24.85
Wednesday	78.70 ± 16.75	93.05 ± 21.75	28.93 ± 8.68	35.30 ± 8.20	59.00 ± 27.45
Thursday	82.03 ± 14.17	90.49 ± 17.88	31.50 ± 9.75	29.94 ± 6.57	58.49 ± 27.94
Friday	79.05 ± 21.29	96.06 ± 13.92	36.52 ± 4.35	33.84 ± 4.48	61.37 ± 26.89
Saturday	74.37 ± 10.19	99.47 ± 21.83	40.92 ± 16.21	31.09 ± 15.45	61.46 ± 27.18
Sunday	61.5 ± 6.86	99.28 ± 21.26	47.28 ± 20.76	36.15 ± 9.15	61.05 ± 23.83

3.2. Spatial Variation

The highest annual average O_3 concentration at the 34 monitoring stations was at the Miyunshuiku Station (75.21 ± 44.36 μg·m^{-3}), followed by that at the Pinggu Station (70.04 ± 49.58 μg·m^{-3}) (Figure 5). The lowest mean value was at the Dongsihuan Station

(45.42 ± 45.45 μg·m^{-3}), followed by the Xizhimenbei Station (49.29 ± 41.65 μg·m^{-3}) and the Nansanhuan Station (49.47 ± 44.44 μg·m^{-3}).

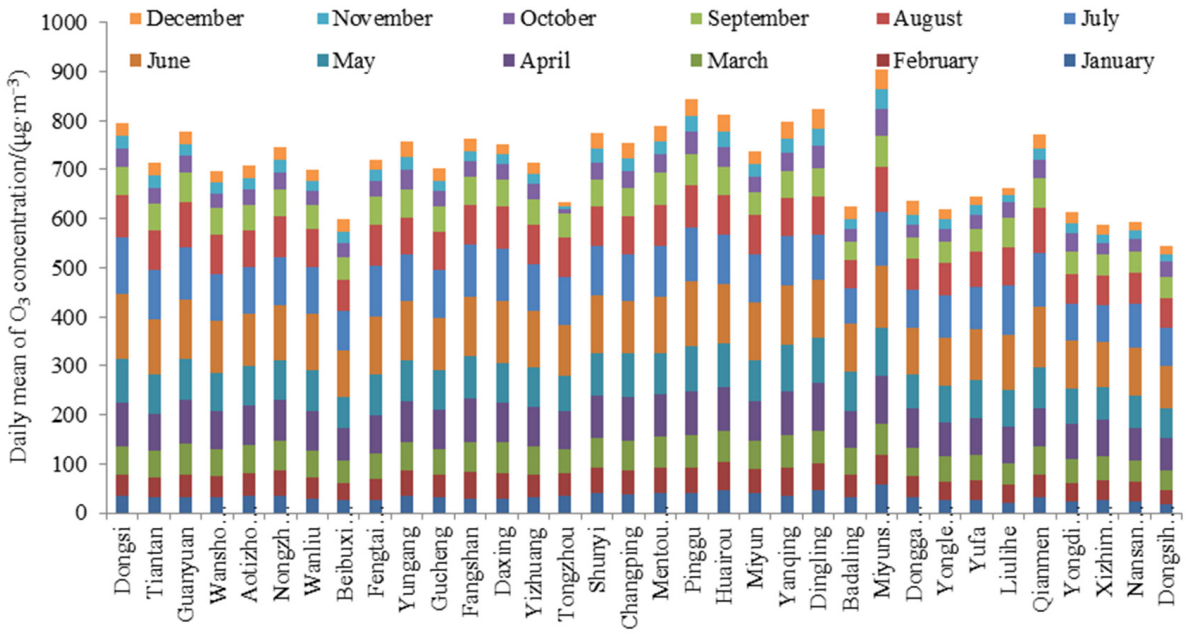

Figure 5. Daily mean of O_3 concentration in each month from the 34 monitoring stations (control station not shown).

Figure 6 shows the distribution of annual mean O_3 concentration at 35 stations fitted using Kriging interpolation. From the perspective of the whole city, the average annual O_3 concentration had slightly higher values in the northeast, southwest and northwest, and slightly lower values in the southeast. The 34 monitoring stations were grouped into six city regions according to their geographical location, i.e., six central districts (1–17); a northwest region (24, 29–31); a northeast region (23, 26–28, 32 and 33); a southwest region (19, 25 and 36); and a southeast region (20–22, 34 and 35). The values of the annual average O_3 concentrations in the six regions were ranked as follows: northeast region (65.37 ± 24.68 μg·m^{-3}) > northwest region (62.54 ± 23.21 μg·m^{-3}) > southwest region (61.53 ± 27.05 μg·m^{-3}) > central six districts (57.33 ± 25.06 μg·m^{-3}). By administrative area, the Miyun District had the highest annual average O_3 concentration, which was 29.52% higher than that of the Haidian District. On the whole, annual average O_3 concentrations in Beijing were higher in the suburbs than in central areas.

The spatial distribution of O_3 changes with different seasons. The highest seasonal average O_3 concentration in spring (Table 2) was in the northwest region (79.62 ± 6.03 μg·m^{-3}). However, the highest seasonal average value in summer was in the southwest region (100.2 ± 6.24 μg·m^{-3}). The highest seasonal average O_3 concentrations in autumn and winter were in the northeast region (41.29 ± 7.75 and 42.45 ± 5.81 μg·m^{-3}, respectively). The seasonal average O_3 concentration in the southwest region showed the greatest difference between seasons.

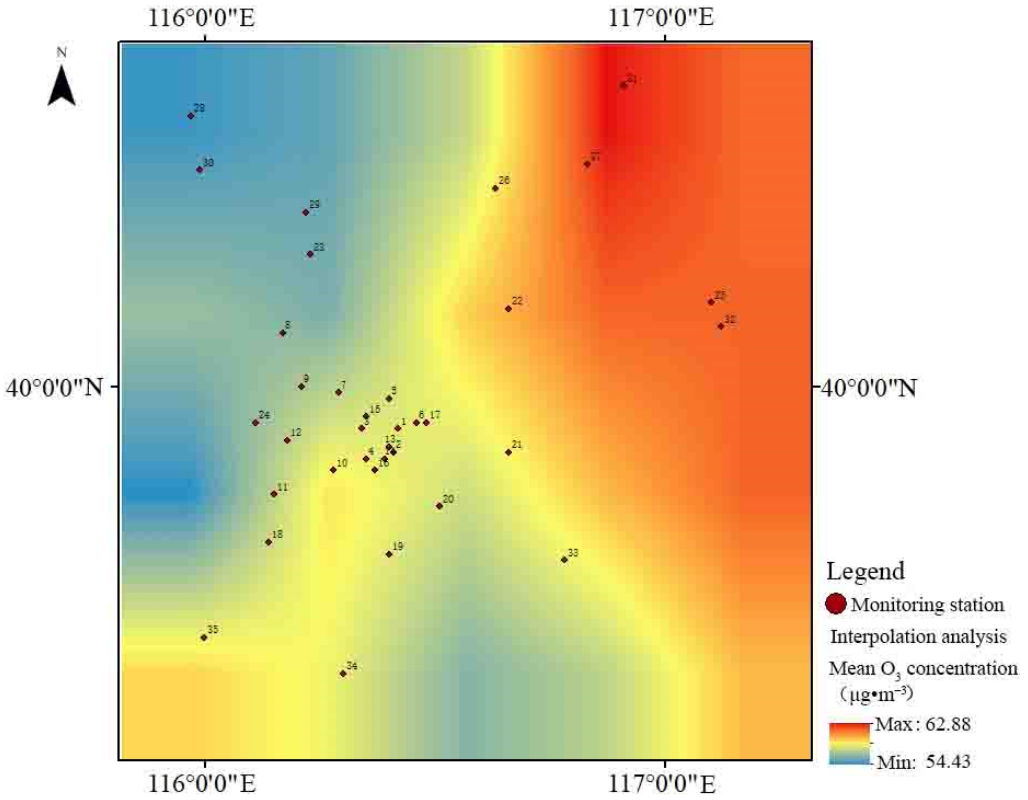

Figure 6. Interpolated (Krigging) contoured surface of annual mean O_3 concentrations in Beijing in 2020.

Table 2. Regional distribution of average seasonal and annual average O_3 concentrations ($\mu g \cdot m^{-3}$).

Region	Spring	Summer	Autumn	Winter	Annual Mean
6 central city districts	69.08 ± 6.87	92.76 ± 11.29	35.35 ± 3.70	32.11 ± 3.98	57.33 ± 25.06
Northwest	79.62 ± 6.03	91.14 ± 9.34	38.63 ± 6.56	40.79 ± 4.29	62.55 ± 23.21
Northeast	78.25 ± 5.78	99.5 ± 10.24	41.29 ± 7.75	42.45 ± 5.81	65.37 ± 24.68
Southwest	73.42 ± 7.04	100.2 ± 6.24	38.69 ± 2.70	33.8 ± 3.31	61.53 ± 27.05
Southeast	69.31 ± 4.00	93.67 ± 7.69	30.72 ± 5.22	30.64 ± 2.78	56.09 ± 26.83

3.3. Correlation between O_3 Concentration and Meteorological Factors

The daily meteorological data are summarized in Figure 7. No significant correlation was found between O_3 concentration and precipitation ($p > 0.05$. Table 3), but there were significant correlations between O_3 concentration and average wind speed, sunshine hours and temperature ($p < 0.05$). The correlation between O_3 concentration and average wind speed was relatively weak, while the highest correlation was between O_3 concentration and daily maximum temperature.

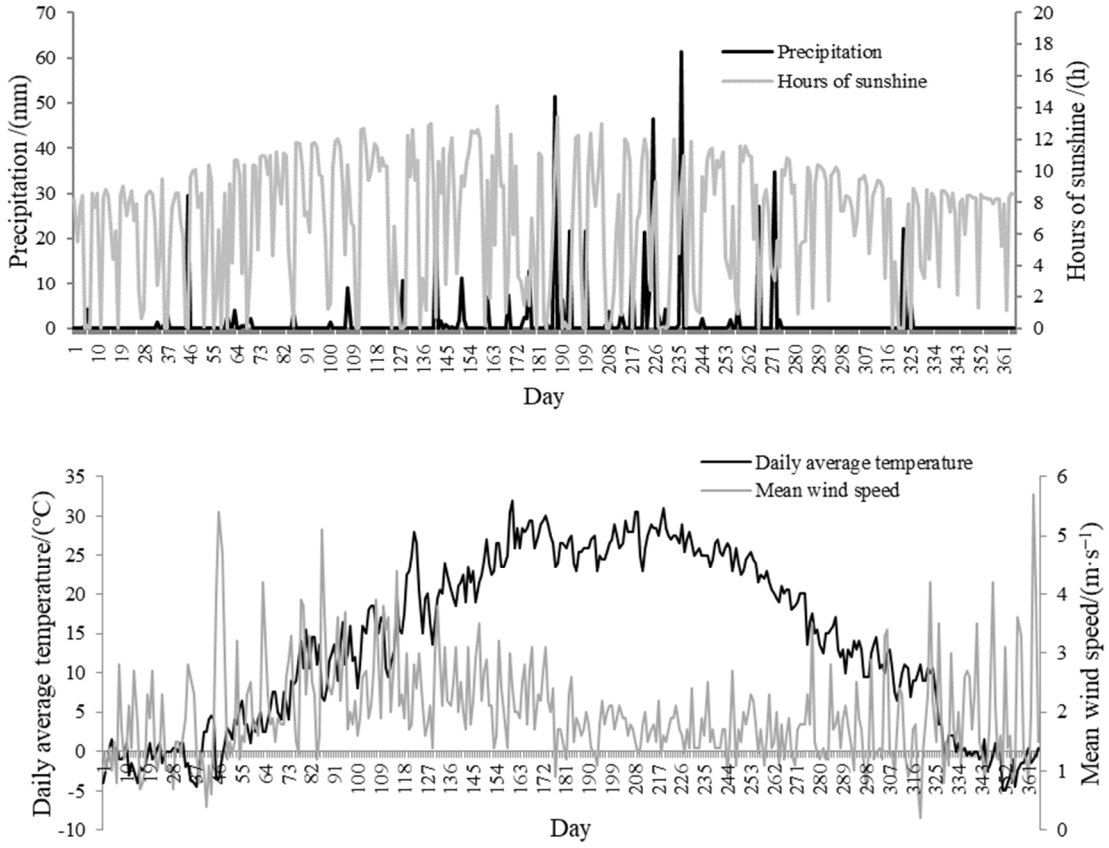

Figure 7. Summary of daily meteorological data. **Upper** figure: Daily precipitation and daily sunshine hours. **Lower** figure: Daily average temperature and daily average wind speed.

With increasing precipitation and sunshine hours (Figure 8), the O_3 concentration decreased at first and then increased. When daily precipitation was in the range 50–60 mm, the daily average value of O_3 concentration was the highest (99.41 $\mu g \cdot m^{-3}$). Contrarily, the daily average O_3 concentration was the lowest (37.17 $\mu g \cdot m^{-3}$) when the daily precipitation was in the range 30–35 mm. When daily sunshine hours were more than 13 h, the daily average value O_3 concentration was highest (95.72 $\mu g \cdot m^{-3}$). With increasing wind speed, the O_3 concentration first increased and then slowly decreased, with the rising rate being greater than the falling rate. When the wind speed was 2.5–3.0 $m \cdot s^{-1}$, the daily average O_3 concentration reached the maximum value (75.32 $\mu g \cdot m^{-3}$). With increasing temperature, the average O_3 concentration also increased. When the temperature was higher than 35 °C, the average value of O_3 concentration was the highest (119.12 $\mu g \cdot m^{-3}$). When the highest temperature was between 0 and 5 °C and the lowest temperature was between 10 and 5 °C, the average value of O_3 concentration reached the lowest values (30.68 and 32.99 $\mu g \cdot m^{-3}$, respectively). From the trend of temperature change throughout the year (Figure 8), higher temperature values in Beijing appeared from May to October, which is consistent with the trend of O_3 concentration. From these results, it is clear that temperature is one of the more important factors affecting O_3 concentration in Beijing.

Table 3. Correlations between O_3 concentration and meteorological factors.

Meteorological Factor	Correlation Coefficient	Significance
Precipitation	0.071	0.178
Mean wind speed	0.267	0.000
Hours of sunshine	0.158	0.003
Maximum temperature	0.724	0.000
Minimum temperature	0.703	0.000

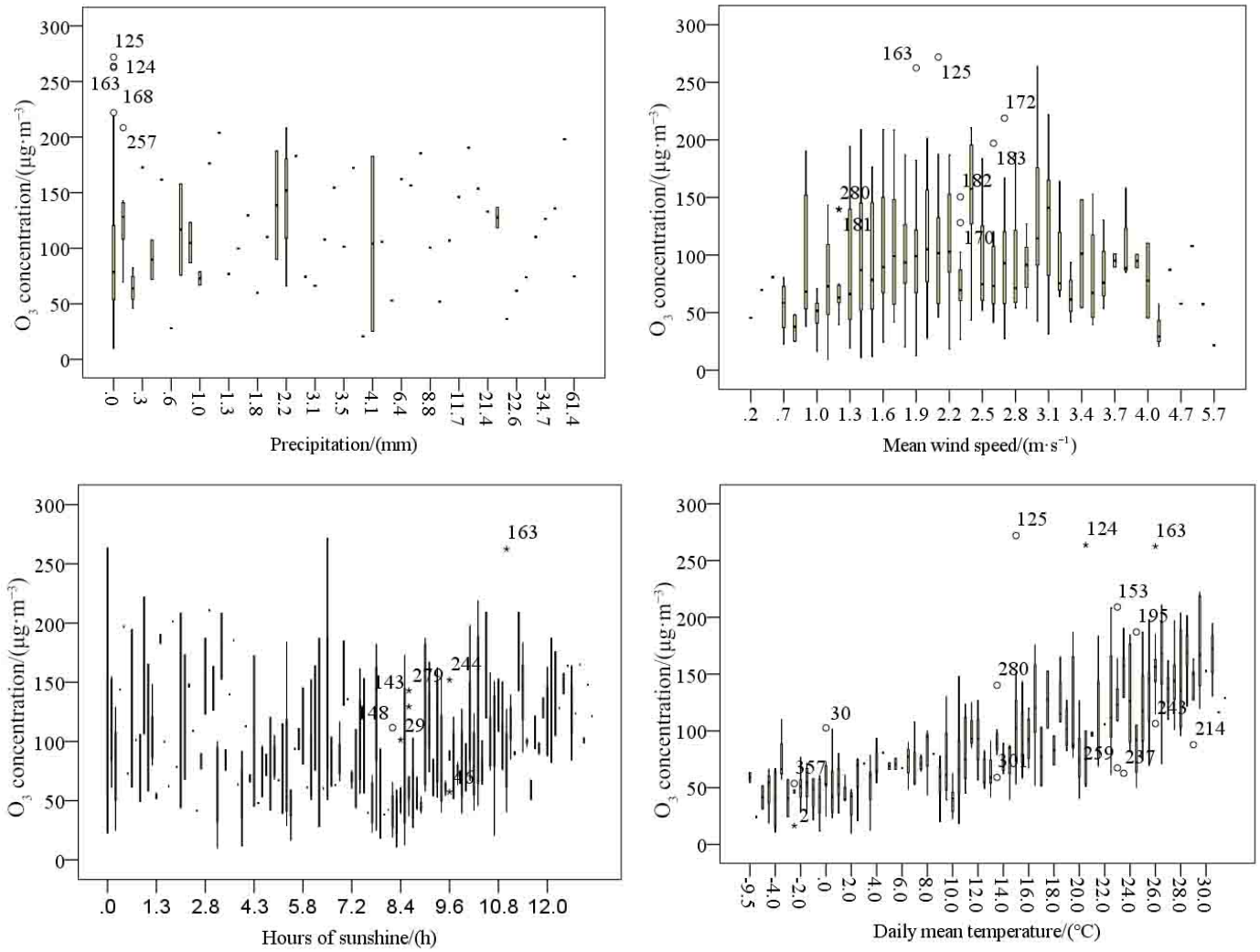

Figure 8. O_3 concentration corresponding to different meteorological factors.

3.4. Correlation between O_3 Concentration and Other Pollutants

As the product of the photochemical reaction, the concentration of O_3 is closely related to other polluting gases in the atmosphere. In 2020, there was a significant negative correlation between O_3 concentrations and NO_2 concentrations and CO concentrations in Beijing (Table 4, $p < 0.001$), with correlation coefficients of −0.553 and −0.159, respectively. There was a significant positive correlation with SO_2 concentration ($0.001 < p < 0.05$).

Table 4. Correlation analysis between O_3 concentration and pollutants.

Pollutant	Correlation	Significance
SO_2	0.031	0.004
NO_2	−0.553	0.000
CO	−0.159	0.000

The correlation between O_3 and its precursor NO_2 is shown in Figure 9. Monthly average values of O_3 concentration show a trend of first increasing and then decreasing through the year, reaching a maximum value in June, followed by July, and lowest value in November. However, the concentration of monthly average NO_2 concentration decreases first and then increases, reaching a minimum in July and a maximum in November. This appears to be related to the requirement for winter heating in Beijing.

In terms of diurnal variation, hourly O_3 concentrations decreased through the night, gradually increased after sunrise, then reached a peak at 16:00 local time, falling back to a minimum at 06:00. However, the hourly NO_2 concentration increased slowly at night and remained at a relatively stable high value until about 08:00, when it gradually decreased to the lowest value at 14:00. These trends are most likely due to the photochemical properties of the two gases. As the solar radiation disappears at night, the ground radiation is weak, and the temperature decreases. NO_2 gradually accumulates until the solar radiation increases after sunrise, when NO_2 gradually decomposes and is consumed, and the O_3 content increases.

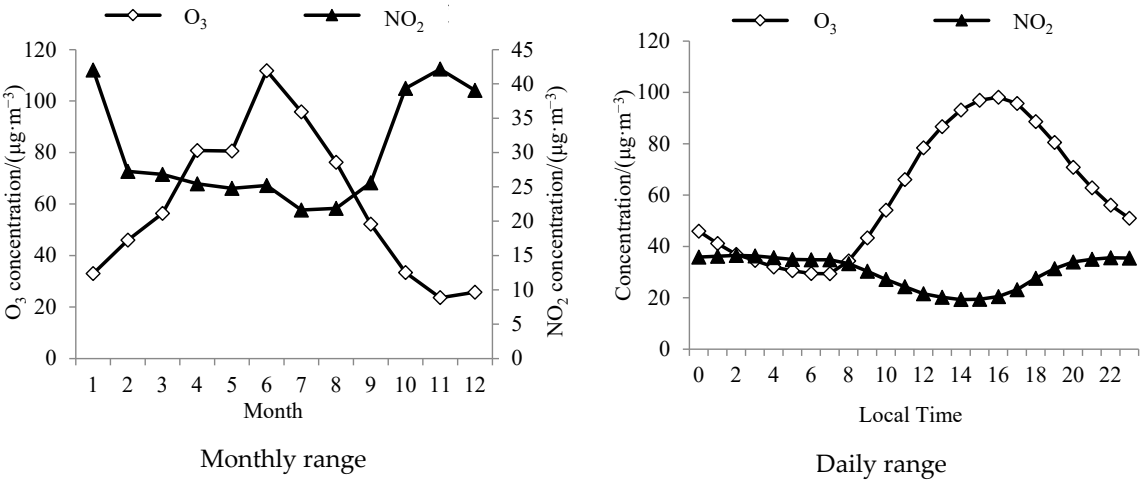

Figure 9. Annual (monthly averages) and daily (hourly values) variations in O_3 and NO_2 concentrations.

4. Discussion

4.1. Spatial-Temporal Dynamic Pattern of O_3 Pollution

According to the statistics of the Bureau of Ecology and Environment, the average values of the maximum 8 h sliding average O_3 concentration from 2016 to 2019 were 190, 193, 192 and 191 $\mu g \cdot m^{-3}$, respectively. Compared with the past 4 years, the O_3 concentrations were lower in 2020, but the annual average was still high. On a seasonal scale, the seasonal variation of O_3 concentration was remarkable, with the highest values in summer and the lowest in winter. On a daily time scale, the O_3 concentration showed a single peak between 13:00 and 18:00.

The most important influencing factor of seasonal and daily variations was temperature. Previous research has shown that the higher the temperature, the higher the O_3 concentration generally [31], which is most clear in the daily variation [32]. The highest values of O_3 concentration observed in Beijing in this study in a day were in the afternoon, corresponding to the period of highest temperature, and gradually decreased with cooling nighttime temperatures.

In terms of annual variation, the highest values of O_3 concentration appeared in June, followed by July. On the one hand, the average temperature in Beijing in June 2020 reached 27.12 °C, which was higher than that in July and August (26.56 and 26.51 °C, respectively), indicating that there was a certain correlation between temperature and O_3 concentration. On the other hand, O_3 concentrations were also related to the shortening of sunshine hours caused by rainy weather in July, August and September. With the shortening of sunshine hours and the decrease in solar radiation, the photochemical reactions of nitrogen oxides (NO_x) and volatile organic compounds (VOC_s) slow down. Southeast winds prevail in summer, compared to the clean air mass from Mongolia in winter, and these winds are more likely to be polluted by the production in eastern cities with high population density.

In terms of weekly variation, Cleveland first put forward the concept of a "weekend effect" in the variation of daily O_3 concentrations, suggesting that the concentration level

of some O_3 precursors (such as VOC_s, CO and NO_x) decreased at the weekend but the concentration of O_3 increased significantly [33]. On a weekly time scale, the daily O_3 average concentrations in Beijing showed a certain weekend effect, with slightly higher values than during weekdays. This is consistent with many existing research results on the weekly variation of O_3 [34,35]. Shi Yuzhen suggested that the reason for the O_3 "weekend effect" in Beijing is that the concentration of NO_x in weekend mornings is lower than that during working days [36].

In terms of spatial distribution, O_3 in Beijing showed different characteristics from other pollutants, such as NO_2, $PM_{2.5}$ and PM_{10}. Geographically, O_3 concentrations were higher in the north and southwest and lowest in the southeast. From the perspective of urban development, concentration values were characterized by being lower in urban areas and higher in the suburbs. This dual pattern distribution was mainly due to the fact that volatile organic compounds can be roughly divided into natural sources and human-made sources, and more than 65% of non-methane volatile organic compounds in the world come from plant-based emissions every year [37]. Some studies have pointed out that the quantities of plant-derived volatile organic compounds (BVOCs) emitted from the Miyun, Yanqing and Changping districts are the highest, together accounting for 35.23% of the city's emissions [38]. BVOCs are one of the important precursors of O_3, and so the O_3 concentration remained high in the former region, while the concentration in the southeast region was low.

The emission of volatile organic compounds from human-made sources is higher in urban areas, but the O_3 concentration is lower than that in suburban areas, which may be related to the consumption of O_3 by NO_2 emissions [39]. In addition, the spatial pattern of O_3 distribution may also be related to the topography and prevailing wind direction of Beijing. Based on the analysis of the topographic elevation data of Beijing and the spatial location of monitoring points, it is found that the O_3 concentration is low in the flat and open areas in the southeast, while the northern areas, especially the Miyun and Huairou areas, are in relatively closed terrain, which makes it difficult for O_3 to spread. According to the statistics of wind direction, the frequency of southwestern wind is very high in spring, summer and autumn. When Beijing is under the influence of southerly winds and westerly winds, the O_3 concentration is relatively high in the north and east of the city. This is because the precursors from the south of Beijing are transported to the northeast.

4.2. Relationship between O_3 Concentration and Meteorological Factors and Other Pollutants

There was a significant positive correlation ($p < 0.001$) between the O_3 concentration and temperature and wind speed. It is concluded that the annual average correlation coefficients of O_3, NO, NO_2 and CO volume fraction and wind speed in Beijing were 0.49, −0.41, −0.49 and −0.38, respectively, although only O_3 was significantly correlated with wind speed [40]. The correlation with temperature was the highest. When temperature increases, the ultraviolet intensity increases, and so the temperature is an important condition for O_3 generation.

Wind speed affects the O_3 concentration in Beijing. Higher wind speeds imply greater air pressure differences between adjacent areas, and strong vertical turbulence often occurs. Higher wind speed changes the surface air pressure. Fast wind will raise the height of the atmospheric boundary layer, causing upper O_3 to flow to the ground. At the same time, higher wind speed also diffuses surface O_3. The turbulent exchange between upper and lower atmospheric layers results in the wind speed being positively correlated with near-surface O_3, while horizontal diffusion makes them negatively correlated [41].

There was a significant correlation between O_3 concentration and sunshine hours in Beijing ($p < 0.05$), but no significant correlation between O_3 concentration and precipitation ($p > 0.05$). The long sunshine hours give sufficient radiation for chemical reactions involving NO_x and VOC_s. Seasonal variation in O_3 concentration is closely related to that of temperature, sunshine hours and wind speed, while daily temperature variation and

human production activities affect the O_3 concentration during a day, and the influence of human activities is the most prominent in the weekly variation.

Wind direction and human activities have a great influence on the spatial variation. When the southeast, south and west wind prevails in Beijing, it is easy to cause high O_3 pollution [40,42]. North airflow comes from Inner Mongolia and generally represents clean air. Southeast airflow comes from Bohai Bay, it originally belonged to a relatively clean ocean air mass, but before reaching Beijing, it was affected by severe air pollution in Tangshan and other cities.

In 2020, there was a significant correlation between O_3 concentration, NO_2 concentration and CO concentration in Beijing ($p < 0.001$) and SO_2 concentration ($0.001 < p > 0.05$). The correlation between O_3 concentration and NO_2 was the highest (-0.553), and there was a significant negative correlation between daily variation and monthly variation. This is consistent with previous analyses of long-term monitoring [43,44], which suggests that O_3 is closely related to NO_2, and the accumulation and decomposition of NO_2 has a very important influence on the formation of O_3 [15].

4.3. Source and Prevention of O_3 Pollution

O_3 pollution is a kind of secondary pollution, and its precursors are mainly NO_x and VOC_s. NO_x is mainly a human-made emission, mostly from automobile exhaust and the combustion of coal and oil, as well as a little from natural lightning. VOC_s have two sources, natural and human-made. Natural sources include volatile organic compounds released by plants, which sometimes leads to high O_3 concentrations in places with lush forest vegetation. Human-made sources include VOCs emitted from various human production activities, such as the coal-based chemical industry, the petrochemical industry, fuel coating manufacturing and solvent manufacturing. Volatile organic compounds emitted from human-made sources are the main causes of urban photochemical pollution [45].

O_3 pollution, although closely related to temperature, sunshine hours and wind speed under specific conditions, is also affected by human activities, which can influence the daily and weekly variations of O_3. In addition to local photochemical smog, pollutants in the surrounding areas also affect the O_3 concentration in Beijing along with the long-distance input of air flow. Under the influence of air flow from the southeast, south and west, polluted air flow from Tianjin, Hebei and other places will also gather here. A simulation study of O_3 pollution in Beijing by Streets [46] found that the contribution of pollution sources from surrounding areas to O_3 concentrations in Beijing is between 35% and 60%.

At present, the prevention and control of O_3 pollution in Beijing mainly focuses on monitoring, early warning and controlling the emission of precursors. As O_3 is an imperceptible pollution, monitoring and early warning of ozone play a very important societal role. It is also necessary to effectively control the emission of volatile organic compounds and nitrogen oxides, such as using clean energy, controlling the number of motor vehicles, improving industrial processes and promoting clean production. As the relationship between O_3 and NO_x and VOC_s is further demonstrated, the emission reduction of NO_x and VOC_s should be verified through studies and more efficient prevention and control measures implemented. As O_3 is transported between regions, the prevention and control of O_3 pollution need to develop from local control to regional joint prevention and control.

5. Conclusions

(1) The annual average daily maximum 8 h distribution was wave-shaped, and the seasonal variation and daily variation were single-peak distributions, with the highest average concentration in June and the highest single-day value between 13:00 and 18:00, with a significant weekly cycle.

(2) The spatial distribution was characterized by high values in the north and low values in the south, with the highest O_3 concentrations in the northeast, the lowest in the southeast and the most significant seasonal change in the southwest. The Miyun District had the highest concentrations and the Haidian District had the lowest con-

centrations. The O_3 concentrations in six central city districts were generally lower than those in the suburbs.

(3) There was no significant correlation between O_3 concentration and precipitation ($p > 0.05$). The correlations between ozone concentration and sunshine hours, wind speed, maximum temperature and minimum temperature were 0.158, 0.267, 0.724 and 0.703, respectively. O_3 concentration was significantly correlated with NO_2 and CO concentration ($p < 0.001$) and significantly correlated with SO_2. The correlation coefficient with NO_2 was the highest and was −0.553. These pollutants showed significant opposite trends in daily variation and monthly variation. When the precipitation is in the range of 50–60 mm, the sunshine hours > 13 h, the wind speed is 2.5–3.0 $m \cdot s^{-1}$ and the temperature is greater than 35 °C, the O_3 concentration will increase.

Author Contributions: Conceptualization, B.C. and X.Y.; methodology, B.C. and X.Y.; software, B.C. and J.X.; validation, B.C. and J.X.; writing—original draft preparation, B.C. and J.; writing—review and editing, B.C. and X.Y.; supervision, B.C. and X.Y.; funding acquisition, B.C. All authors have read and agreed to the published version of the manuscript.

Funding: This work was supported by Youth fund of Beijing Academy of Agricultural and Foestry Sciences(QNJJ202017), President fund of Institute of Forestry and Pomology (201903), and National Natural Science Foundation of China (31500352).

Conflicts of Interest: The authors declare no conflict of interest.

References

1. Vingarzan, R. A review of surface ozone background levels and trends. *Atmos. Environ.* **2004**, *38*, 3431–3442. [CrossRef]
2. Wang, T.; Xue, L.K.; Brimblecombe, P.; Lam, Y.F.; Li, L.; Zhang, L. Ozone pollution in China: A review of concentrations, meteorological influences, chemical precursors, and effects. *Sci. Total Environ.* **2017**, *575*, 1582–1596. [CrossRef] [PubMed]
3. Lin, N.; Jiang, R.F.; He, Y.H.; Ren, S.S.; Zhuang, X.Y. A case study of ozone pollution in Putian. *Acta Sci. Circumstantiae* **2021**, *41*, 2569–2576.
4. Zhang, H.X.; Sun, X.; Yao, Y.H.; Wan, W.X.; Xiao, Y.; Sun, B.F.; William, J.M.; Han, C.M.; Gao, S.Q.; Gao, F.Y.; et al. Ground-level ozone distribution pattern in summer of Beijing and its foliar injury effect upon plants. *Acta Ecol. Sin.* **2014**, *34*, 4756–4765.
5. Chen, B. *Effects of Ozone Stress on the Growth and Physiological Characteristics of Four Tree Species*; Beijing Forestry University: Beijing, China, 2018.
6. Chen, Z.; Yu, H.; Shang, H.; Cao, J.X. Effects of Ozone Stress on Tree Root: A Review. *For. Res.* **2016**, *29*, 455–463.
7. Wu, K.; Kang, P.; Yu, L.; Gu, S.; Wen, X.H.; Wang, Z.S.; Chen, Y.Z.; Chen, S.Y.; Zhao, S.Q.; Wang, H.L.; et al. Pollution status and spatiotemporal variations of ozone in China during 2015–2016. *Acta Sci. Circumstantiae* **2018**, *38*, 2179–2190.
8. Wang, X.; Mauzerall, D.L. Characterizing distributions of surface ozone and its impact on grain production in China, Japan and South Korea: 1990 and 2020. *Atmos. Environ.* **2004**, *38*, 4383–4402. [CrossRef]
9. Ma, J.Z.; Chu, B.W.; Liu, J.; Liu, Y.C.; He, H.; Zhang, H.X. NOx promotion of SO_2 conversion to sulfate: An important mechanism for the occurrence of heavy haze during winter in Beijing. *Environ. Pollut.* **2018**, *233*, 662–669. [CrossRef]
10. Yang, Y.R.; Liu, X.G.; Qu, Y.; Wang, J.L.; An, J.L.; Zhang, Y.; Zhang, F. Formation mechanism of continuous extreme haze episodes in the megacity Beijing, China, in January 2013. *Atmos. Res.* **2015**, *155*, 192–203. [CrossRef]
11. Ministry of Ecology and Environment. *China Environmental Statement 2019*; Ministry of Ecology and Environment: Beijing, China, 2020.
12. Lu, J.; Huang, C.; Wang, H.L.; Wang, Q.; Yan, R.S.; Jing, S.A. Scientific understanding of ozone pollution and history of its control in the United States. *Environ. Pollut. Control* **2020**, *42*, 1171–1175.
13. Xu, Y.S.; Wen, X.M.; Miao, G.B. Ozone Pollution and its Control Countermeasures. *China Environ. Prot. Ind.* **2018**, *6*, 35–38.
14. Wang, Z.S.; Li, Y.T.; Chen, T.; Zhang, D.W.; Sun, F.; Sun, R.W.; Dong, X.; Sun, N.D.; Pan, L.B. Temporal and Spatial Distribution Characteristics of Ozone in Beijing. *Environ. Sci.* **2014**, *35*, 4446–4453.
15. Fu, C.Z.; Zhou, H. Research Progress on the Formation Mechanism and Impact Factors of Urban Ozone Pollution in China. *Environ. Monit. China* **2014**, *35*, 4446–4453.
16. Ma, Z.Q.; Wang, Y.S.; Zhang, X.L.; Xu, J. Comparison of Ozone Between Beijing and Downstream Area. *Environ. Sci.* **2011**, *32*, 924–929.
17. Wang, Z.F.; Li, L.N.; Wu, Q.Z.; Gao, C.; Li, X. Simulation of the Impacts of Regional Transport on Summer Ozone Levels Over Beijing. *Chin. J. Nat.* **2008**, *30*, 194–198.
18. Tang, G.; Li, X.; Wang, Y.; Xin, J.; Ren, X. Surface ozone trend details and interpretations in Beijing 2001–2006. *Atmos. Chem. Phys.* **2009**, *9*, 8813–8823. [CrossRef]

19. Xu, J.; Ma, J.Z.; Zhang, X.L.; Xu, X.B.; Xu, X.F.; Lin, W.L.; Wang, Y.; Meng, W.; Ma, Z.Q. Measurements of ozone and its precursors in Beijing during summertime: Impact of urban plumes on ozone pollution in downwind rural areas. *Atmos. Chem. Phys.* **2011**, *11*, 12241–12252. [CrossRef]
20. Huang, A.K.; Li, N. The ecological significance of botanical volatile organic compounds. *Subtrop. Plant Sci.* **2011**, *40*, 81–86.
21. Tang, G.Q.; Li, X.; Wang, X.K.; Xin, J.Y.; Hu, B.; Wang, L.L.; Wang, X.K.; Ren, Y.F.; Wang, Y.S. Effects of synoptic type on surface ozone pollution in Beijing. *Environ. Sci.* **2010**, *31*, 6814.
22. Tang, H.Y.; Liu, G.; Zhu, J.G.; Han, Y.; Kobayashi, K. Seasonal variations in surface ozone as influenced by Asian summer monsoon and biomass burning in agricultural fields of the northern Yangtze River Delta. *Atmos. Res.* **2013**, *122*, 67–76. [CrossRef]
23. Marr, L.C.; Harley, R.A. Spectral analysis of weekday–weekend differences in ambient ozone, nitrogen oxide, and non-methane hydrocarbon time series in California. *Atmos. Environ.* **2002**, *36*, 2327–2335. [CrossRef]
24. Pollack, I.B.; Ryerson, T.B.; Trainer, M.; Neuman, J.A.; Roberts, J.M.; Parrish, D.D. Trends in ozone, its precursors, and related secondary oxidation products in Los Angeles, California: A synthesis of measurements from 1960 to 2010. *J. Geophys. Res. Atmos.* **2013**, *118*, 5893–5911. [CrossRef]
25. Kheirbek, I.; Wheeler, K.; Walters, S.; Kass, D.; Matte, T. $PM_{2.5}$ and ozone health impacts and disparities in New York City: Sensitivity to spatial and temporal resolution. *Air Qual. Atmos. Health* **2013**, *6*, 473–486. [CrossRef] [PubMed]
26. Fujita, E.M.; Stockwell, W.R.; Campbell, D.E.; Keislar, C.E.; Lawson, D.R. Evolution of the magnitude and spatial extent of the weekend ozone effect in California's South Coast Air Basin, 1981–2000. *J. Air Waste Manag. Assoc.* **2003**, *53*, 802–815. [CrossRef]
27. Cheng, N.L.; Li, Y.T.; Zhang, D.W.; Chen, T.; Wang, X.; Huan, N.; Chen, C.; Meng, F. Characteristics of ozone over standard and its relationships with meteorological conditions in Beijing city in 2014. *Environ. Sci.* **2016**, *37*, 2041–2051.
28. Jia, H.Y.; Yi, T.; Qu, X.; Cheng, N.L.; Chen, B.F.; Wang, J.K.; Tang, J.K.; Tang, W.; Meng, F.; Chai, F.H. Characteristics and source simulation of ozone in Beijing and its surrounding areas in 2015. *China Environ. Sci.* **2017**, *37*, 1231–1238.
29. Cheng, L.J.; Wang, S.H.; Gong, Z.Y.; Yang, Q.; Wang, Y.Y. Spatial and seasonal variation and regionalization of ozone concentrations in China. *China Environ. Sci.* **2017**, *37*, 4003–4012.
30. *GB/T 3095—2012*; Ambient Air Quality Standard. Ministry of Environmental Protection of the People's Republic of China, Standards Press of China: Beijing, China,, 2012.
31. Cui, M.G.; Bai, L.Y.; Feng, J.Z.; Lin, X.S.; Li, H.L.; Gao, W.W.; Li, Z.W. Analysis of temporal and spatial variations of ozone coupling with dynamics of meteorological factors in the Beijing-Tianjin-Tangshan region. *Acta Sci. Circumstantiae* **2021**, *41*, 374–385.
32. Cheng, N.L.; Li, Y.T.; Zhang, D.W.; Chen, T.; Wei, Q.; Sun, T.H.; Wang, B.Y.; Fu, J.M.; He, L.W.; Cheng, B.F.; et al. Characteristics of ozone background concentration in Beijing from 2004 to 2015. *Environ. Sci.* **2016**, *37*, 2847–2854.
33. Cleveland, W.S.; Graedel, T.E.; Kleiner, B.; Warner, J.L. Sunday and workday variations in photochemical air pollutants in New Jersey and New York. *Science* **1974**, *186*, 1037–1038. [CrossRef]
34. Yin, Y.Q.; Shan, W.P.; Ji, X.; You, L.N.; Su, Y.C. Characteristics of Atmospheric Ozone in the Urban Area of Ji'nan. *Environ. Sci.* **2006**, *27*, 2299–2302.
35. Tang, W.Y.; Zhao, C.S.; Geng, F.H.; Peng, L.; Zhou, G.Q.; Gao, W.; Xu, J.M. Study of ozone "weekend effect" in Shanghai. *Sci. Sin.* **2009**, *39*, 99–105. [CrossRef]
36. Shi, Y.Z.; Xu, Y.F.; Wang, G.C.; Shi, L.Q. Study of the "Weekend Effect" of O_3, NO_x and Other Pollutants in Summer of Beijing. *Environ. Sci.* **2009**, *30*, 2832–2838.
37. Shao, M.; Dong, D. Pollution and control of atmospheric volatile organic compound in China. *Environ. Prot.* **2013**, *41*, 25–28.
38. Jing, X.X. *Study on Biogenic Volatile Organic Compounds Emission from Forest Plants in Beijing*; Beijing Forestry University: Beijing, China, 2020.
39. Sillman, S.; Logan, J.A.; Wofsy, S.C. The sensitivity of ozone to nitrogen oxides and hydrocarbons in regional ozone episodes. *J. Geophys. Res.* **1990**, *95*, 1837–1851. [CrossRef]
40. An, J.L.; Wang, Y.S.; Sun, Y. Assessment of ozone variations and meteorological effects in Beijing. *Ecol. Environ. Sci.* **2009**, *18*, 944–951.
41. Yan, R.S.; Chen, M.D.; Gao, Q.X.; Liu, T.; Hu, S.X.; Gao, W.K. Characteristics of typical ozone pollution distribution and impact factors in Beijing in summer. *Res. Environ. Sci.* **2013**, *26*, 43–49.
42. Xu, J.; Zhang, X.L.; Zhao, X.J.; Xu, X.F.; Meng, W. Influence of summer local circulation on the transportation of ozone from urban to the downwind area in Beijing. *China Environ. Sci.* **2009**, *29*, 1140–1146.
43. Chen, P.F.; Zhang, Q.; Quan, J.N.; Gao, Y.; Huang, M.Y. Temporal and spatial distribution of ozone concentration by aircraft sounding over Beijing. *Environ. Sci.* **2012**, *33*, 4141–4150.
44. Cui, M.; An, X.Q.; Sun, Z.B.; Wang, B.Z.; Wang, C.; Ren, W.H.; Li, Y.J. Characteristics and meteorological conditions of ozone pollution in Beijing. *Ecol. Environ. Monit. Three Gorges* **2019**, *4*, 25–35.
45. Yang, F.; Yan, Y.L.; Ge, Y.F.; Li, R.M.; Li, Y.H.; Yu, H.L.; Peng, L. Characteristics and source apportionment of ambient volatile organic compounds in winter in Jincheng. *Environ. Sci.* **2018**, *39*, 4042–4050.
46. Streets, D.G.; Fu, J.S.; Jang, C.J.; Hao, J.M.; He, K.B.; Tang, X.Y.; Zhang, Y.H.; Wang, Z.F.; Li, Z.P.; Zhang, Q.; et al. Air quality during the 2008 Beijing Olympic Games. *Atmos. Environ.* **2007**, *41*, 480–492. [CrossRef]